Journal of Optics B: Quantum and Semiclassical Optics

Multi-hump optical solitons in a saturable medium

To cite this article: Elena A Ostrovskaya and Yuri S Kivshar 1999 *J. Opt. B: Quantum Semiclass. Opt.* **1** 77

Multi-hump optical solitons in a saturable medium

Elena A Ostrovskaya and Yuri S Kivshar

Optical Sciences Centre, Research School of Physical Sciences and Engineering, Australian National University, Canberra 0200, ACT, Australia

Received 17 July 1998, in final form 4 November 1998

Abstract. We investigate multi-hump spatial solitary waves and multi-soliton patterns generated by an incoherent interaction of two optical beams in a medium with saturable (e.g. photorefractive) nonlinearity. Applying a bifurcation analysis and numerical relaxation technique, we reveal different scenarios of creating the multi-hump solitons and find the families of solitary waves composed of two mutually coupled components. We analyse the stability of these solitons to propagation and find that the evolution of a soliton is governed by its modal structure.

Keywords: Multi-hump optical solitons, solitons in photorefractive media, multi-soliton structures

1. Introduction

Spatial optical solitons (or *self-guided optical beams*) [1] have attracted a great deal of attention because of their potential application in ultrafast all-optical switching. When a spatial soliton is composed of more than one beam or polarization component, its structure becomes complex and the soliton intensity profile may display several peaks. These are the so-called *multi-hump optical solitons*, which were recently observed experimentally in a photorefractive medium [2].

Multi-hump soliton states can be created in two ways. The first way, already demonstrated experimentally [2], is when a fundamental (one-hump) soliton created by one beam, is coupled to one (or more) higher-order guided modes of the effective waveguide it induces in a nonlinear medium†. For this to be possible, the power of the fundamental soliton should exceed a certain threshold value defined by the cutoff of the corresponding higher-order mode. The amplitude of the fundamental soliton unambiguously determines the number of guided modes which can be supported by the self-induced soliton waveguide, and therefore, the possible modal structure of a multi-hump soliton. The second way of creating multi-hump solitons is to form a bound state of two (or more) fundamental solitons, again viewed as several guided modes trapped by the soliton waveguides [4]. In our work we show that whenever the formation of the multi-hump solitons follows the latter scenario, it inevitably leads to a structural instability of the resulting beams, even without perturbation. We use the term '*structural instability*' in a sense earlier introduced in [5], which implies a change in the shape of the transverse profile of the beam, without the collapse or decay usually associated with linear instability of one-component solitons [6, 7]. If losses are negligible, the structural instability conserves the total power of the soliton beam. For example, a two-hump soliton formed by a fundamental soliton in one component and a first-order mode in the other component is structurally stable when the amplitude of the second component is small enough. In the case where the corresponding amplitude is no longer small (and therefore the beam is no longer weak), the nonlinear coupling causes deformation of the soliton-induced waveguide. This leads to the fundamental soliton itself acquiring two humps in the intensity profile and being treated as a bound state of two fundamental solitons. The two corresponding waveguides can, in turn, support a number of guided modes. Such a transition from a two-component soliton to a bound state of two solitons was first described for the case of the Kerr-like nonlinearity in [8]. In this paper, we demonstrate that much richer classes of two-component solitons and their bifurcations exist in a saturable medium, such as that used in the experiment [2].

Multi-hump bound states of bright solitons are structurally unstable. Nevertheless, it is the instability that can be employed in a variety of schemes for all-optical switching, provided the intensity and polarization dynamics of the solitons is fairly predictable. In this paper we demonstrate several types of the instability-induced soliton dynamics potentially useful for soliton switching.

† For an excellent overview of the soliton-induced waveguides in a photorefractive medium, see [3].

2. Renormalized equations

We consider incoherent interaction between two linearly-polarized optical beams in a biased photorefractive medium. The model equations for the normalized amplitudes of the beams are [9]:

$$
\begin{aligned}
&\mathrm{i}\frac{\partial U}{\partial Z} + \frac{1}{2}\frac{\partial^2 U}{\partial X^2} - \beta(1+\rho)\frac{U}{1+|U|^2+|W|^2} = 0, \\
&\mathrm{i}\frac{\partial W}{\partial Z} + \frac{1}{2}\frac{\partial^2 W}{\partial X^2} - \beta(1+\rho)\frac{W}{1+|U|^2+|W|^2} = 0.
\end{aligned}
\tag{1}
$$

Here $\rho = I_\infty/I_d$, and $\beta = (k_0x_0)^2 n_e^4 r_{33} E_0/2$, where I_∞ stands for the total power density away from the beam, I_d is the so-called dark irradiance, k_0 is the propagation constant, x_0 is the spatial width of the beam, and $n_e^4 r_{33} E_0$ is a correction to the refractive index due to the external field applied to a crystal along the transverse X-direction [10].

In the case of negative nonlinearity, $\beta < 0$, the system of coupled nonlinear equations (1) possesses families of two-parameter bright solitary waves. To find these solutions, we measure the spatial coordinates Z and X in units of $[\beta(1+\rho)]^{-1}$ and $[\beta(1+\rho)]^{-1/2}$, respectively, and look for the soliton solutions in the form: $U(X,Z) = u(q_1,q_2;X,Z)\mathrm{e}^{\mathrm{i}q_1 Z}$, $W(X,Z) = w(q_1,q_2;X,Z)\mathrm{e}^{\mathrm{i}q_2 Z}$. The task of searching for stationary solutions can be simplified by adopting the following renormalization: $s = 1-q_1$, $u = \sqrt{s}u$, $w = \sqrt{s}u$, $\lambda = (1-q_2)/s$, $x = \sqrt{s}X$, $z = sZ$. Normalized functions u and w then satisfy the following equations:

$$
\begin{aligned}
&\mathrm{i}\frac{\partial u}{\partial z} + \frac{1}{2}\frac{\partial^2 u}{\partial x^2} + \frac{u(|u|^2+|w|^2)}{1+s(|u|^2+|w|^2)} - u = 0, \\
&\mathrm{i}\frac{\partial w}{\partial z} + \frac{1}{2}\frac{\partial^2 w}{\partial x^2} + \frac{w(|u|^2+|w|^2)}{1+s(|u|^2+|w|^2)} - \lambda w = 0
\end{aligned}
\tag{2}
$$

where λ is a *soliton parameter*, and the strength of the mutual coupling of the two components is defined by the *saturation parameter* s.

Stationary solutions of system (2) exist for $\{s,\lambda\} \leqslant 1$. Moreover, in the limit $s \to 0$, system (2) reduces to the exactly solvable *Manakov model* for the solitons in Kerr-type nonlinear media with equal cross- and self-phase modulation coefficients [11]. This limiting case was thoroughly investigated in [5, 12].

3. Bifurcation analysis and stationary solutions

Stationary solutions are given by real, z-independent functions $u(x;\lambda,s)$ and $w(x;\lambda,s)$ satisfying equations (2). In the general case $s \neq 0$, equations (2) possess no analytic solutions. However, some progress can be made by employing a perturbation approach.

First, by setting the amplitude of one of the components equal to zero, we can obtain the simplest one-component solutions of equations (2) defined by a system of decoupled ordinary differential equations for u and w. This system can be integrated once to yield:

$$
\begin{aligned}
&\frac{\mathrm{d}u_0}{\mathrm{d}x} = \pm\frac{\sqrt{2}}{s}\sqrt{\log(1+su_0^2) - s(1-s)u_0^2} \\
&\qquad \text{and} \qquad w \equiv 0, \\
&\text{or} \\
&\frac{\mathrm{d}w_0}{\mathrm{d}x} = \pm\frac{\sqrt{2}}{s}\sqrt{\log(1+sw_0^2) - s(\lambda-s)w_0^2} \\
&\qquad \text{and} \qquad u \equiv 0,
\end{aligned}
\tag{3}
$$

from which the fundamental (one-hump, no-nodes) solitons, $u_0(x)$ and $w_0(x)$, can be found numerically [13]. We use the term '*multi-hump solitons*' to describe stationary two-component solutions (u,w) of the system (2) that have more than one maximum in the transverse intensity profile. They can be found by analysing the possible bifurcations of the fundamental solution $u_0(x)$, when a new solution with both non-zeroth components (u,w) emerges. This solution consists of a mutually coupled fundamental soliton and a higher-order mode of the effective waveguide it induces. The resulting soliton thus has two components and, correspondingly, *two modes*. To find such solitons, we assume that one of the components is extremely small, i.e. $w/u \sim \varepsilon \ll 1$. To first order in ε, the first equation of system (2) produces the fundamental solution, $u_0(x)$. The second equation transforms into a self-consistent, *linear* Schrödinger equation:

$$
\frac{\mathrm{d}^2 w}{\mathrm{d}x^2} + 2\{W(x) - \lambda\}w = 0,
\tag{4}
$$

where the effective potential is defined as $W(x) \equiv u_0^2(x)/[1+su_0^2(x)]$. The eigenfunctions of the eigenvalue problem (4) generate a set of 'modes' of the waveguide $W(x)$ created by the fundamental soliton of the u-component. The modes are conventionally identified by the number of nodes, n. The ground state, or *zeroth-order mode*, of this waveguide has no nodes, $n = 0$. A fundamental soliton can therefore be considered as a zeroth-order mode of the waveguide it induces [4]. The cutoff values $\lambda_n^{(0)}$ for the nth-order modes correspond to bifurcation points for the fundamental soliton, since at any of these points in the space of parameters $\{\lambda, s\}$, a new two-component soliton, consisting of the mutually coupled fundamental (zeroth-order) and one of the higher-order modes, appears.

We should be careful not to extend the concept of the induced waveguide and its linear modes too far. Indeed, the linearized equation (4) is only applicable near the bifurcation points, where the w-component is small compared to the u-component. It is erroneous to use the system of eigenmodes of the linearized equation (4) for the purpose of modal decomposition of *any two-component stationary solution*. As soon as the amplitude of a guided mode becomes large enough the soliton waveguide itself deforms and the transverse profiles of the u and w soliton components no longer correspond to the initial zeroth- and higher-order modes, even though they preserve the number of nodes. Such a mutual action of the two soliton components is *a purely nonlinear effect* which, as will be shown below, affects the propagation dynamics of the solitons.

The discrete eigenvalues, $\{\lambda_n\}$, and corresponding eigenfunctions, $\{w_n\}$, of the problem (4) can be found numerically. Additionally, some estimates for the bifurcation points can be obtained using a kind of 'semiclassical' approximation [14]. Since equation (4) closely resembles an eigenvalue equation of nonrelativistic quantum mechanics, the number of localized states, n, should obey the Bohr–Sommerfeld quantization rule:

$$
J(\lambda_n) \equiv \sqrt{2}\int_{x_1}^{x_2} \sqrt{W(x) - \lambda_n}\,\mathrm{d}x = \pi(n + \tfrac{1}{2}),
\tag{5}
$$

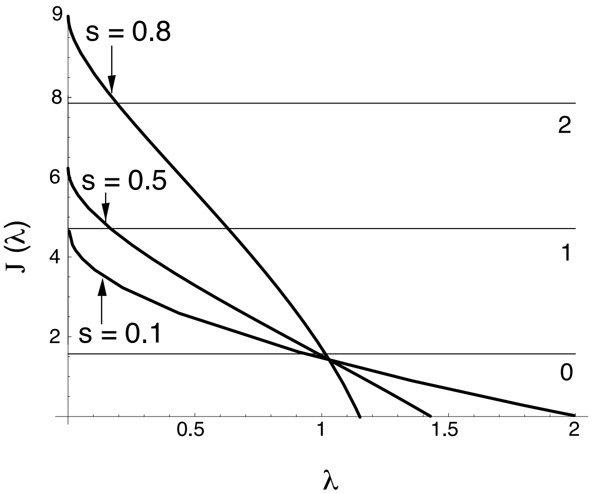

Figure 1. Dependence of the phase integral, $J(\lambda)$, defined by equation (6), on the soliton parameter λ, for three values of the saturation parameter s. Intersection of $J(\lambda)$ with the horizontal line ($n = 0, 1, 2, \ldots$) defines a cutoff for the nth-order mode of the soliton-induced waveguide.

where $J(\lambda)$ is the phase integral between the turning points, x_1 and x_2. By changing the variables, $y = u_0(x)$, we obtain that $\lambda_n(s)$ is given by the integral equation:

$$J(\lambda_n) \equiv \int_{y_1}^{y_2} \frac{2s\sqrt{y^2 - \lambda_n(1 + sy^2)}\,\mathrm{d}y}{\sqrt{(1 + sy^2)[\log(1 + sy^2) - s(1 - s)y^2]}} = \pi\left(n + \frac{1}{2}\right), \qquad (6)$$

where $y_1 \equiv u_0(x_1) = \sqrt{\lambda_n/(1 - \lambda_n s)}$, and y_2 corresponds to a global minimum of the potential $W(x)$ given by a positive root of the equation: $\log(1 + s{y_2}^2) - s(1 - s){y_2}^2 = 0$.

We then solve the integral equation (6) numerically to find the points of intersection of the function $J(\lambda)$ with the constants $\pi(n + \frac{1}{2})$. Each such intersection defines the approximate cut-off value of the nth mode $\lambda_n^{(0)}$ or, in terms of the primary problem, the bifurcation point of the fundamental solution. The corresponding examples are presented in figure 1, for three different values of the saturation parameter s. As can be seen from figure 1, the effective potential created by a fundamental soliton can support a larger number of modes at larger values of s (see also [3]). We confirmed, by solving equations (2) numerically, that a two-component soliton consisting of a fundamental soliton (in the u-component) and a zeroth-order mode of its effective waveguide (in the w-component), exists only at $\lambda = 1$.

To quantify the validity of the bifurcation analysis we compare the cutoff of the first-order ($n = 1$) mode deduced from equation (6) with that obtained by solving model equations (2) numerically in order to find their stationary localized solutions. The corresponding results are presented in figure 2 by the curves A and B. Some discrepancy between our theory (curve A) and numerics (curve B) stems from the fact that the semiiclassical approximation becomes less accurate for $s \ll 1$.

4. Modal structure of multi-hump solitons

Bifurcations of the fundamental solitons originally created in the u-component give birth to families of stationary two-mode solitons consisting of zeroth and nth modes. Such solitons appear at bifurcation points $\lambda_n^{(0)}(s)$ and exist only for $\lambda(s) \geqslant \lambda_n^{(0)}(s)$. Different types of two-component solitons can be conveniently presented on a bifurcation diagram using the total soliton power, an invariant of the model (2). Soliton power P is defined as

$$P = \int_{-\infty}^{\infty} \{|u(x)|^2 + |w(x)|^2\}\,\mathrm{d}x, \qquad (7)$$

and, for a fixed value of the saturation parameter s, it depends only on the dimensionless soliton parameter λ.

As has been discussed in the previous section, the linear analysis developed in the vicinity of the bifurcation points for a fundamental soliton (u-component) cannot be applied in the case of the large amplitude of a coupled higher-order mode (w-component), i.e. at $\lambda(s) \gg \lambda_n^{(0)}(s)$. However, the whole family of two-mode solitons, characterized by a certain functional dependence $P(\lambda)$, can be found by the numerical relaxation technique. The results of our numerical calculations are presented in figure 3 for different types of multi-hump solitons found at $s = 0.5$.

Importantly, the number of maxima in the total intensity profile of a two-mode soliton *does not uniquely define its modal structure*. In other words, there are various scenarios leading to the formation of multi-hump solitons in the model (2).

For example, figure 3 presents a branch of a two-mode soliton solution, originating at the bifurcation point Q, and consisting of a zeroth (u) and a first-order (w) mode. Amplitude profiles of the two components corresponding to three different points on the soliton branch are presented in figures 2(a)–(c). As can be seen from figures 2(a)–(c), the initial modes deform greatly as we move along the branch of the soliton solutions, away from the point Q. In fact, at any value of s, a two-component soliton consisting of fundamental and first-order modes undergoes deformation of the intensity profile with increasing λ. Critical phases of the deformation are indicated in figure 2 by curves C and D. Close to a bifurcation threshold (curve B) the soliton is single-humped as in figure 2(a). The intensity profile becomes *two-humped* at a considerable distance from the bifurcation point, on the curve C. Increasing λ even further, leads to the increasing intensity of the first-order mode, until it starts deforming the u-mode itself. Mode profiles of figure 2(b) are characteristic for the threshold curve D where the u-component becomes two-humped. And, finally, at the limit $\lambda \to 1$, the intensity humps become largely separated, and the initial waveguide becomes W-shaped, as shown in figure 2(c). In this limit, the soliton can no longer be described as a two-mode structure. Instead, it is conventional to consider both u- and w-components as bound states of two fundamental solitons, in- and out-of-phase, correspondingly [15, 16].

In a similar manner, we can find families of solitons composed of a zeroth- and second-order mode that originate at the second bifurcation point, when the soliton-induced

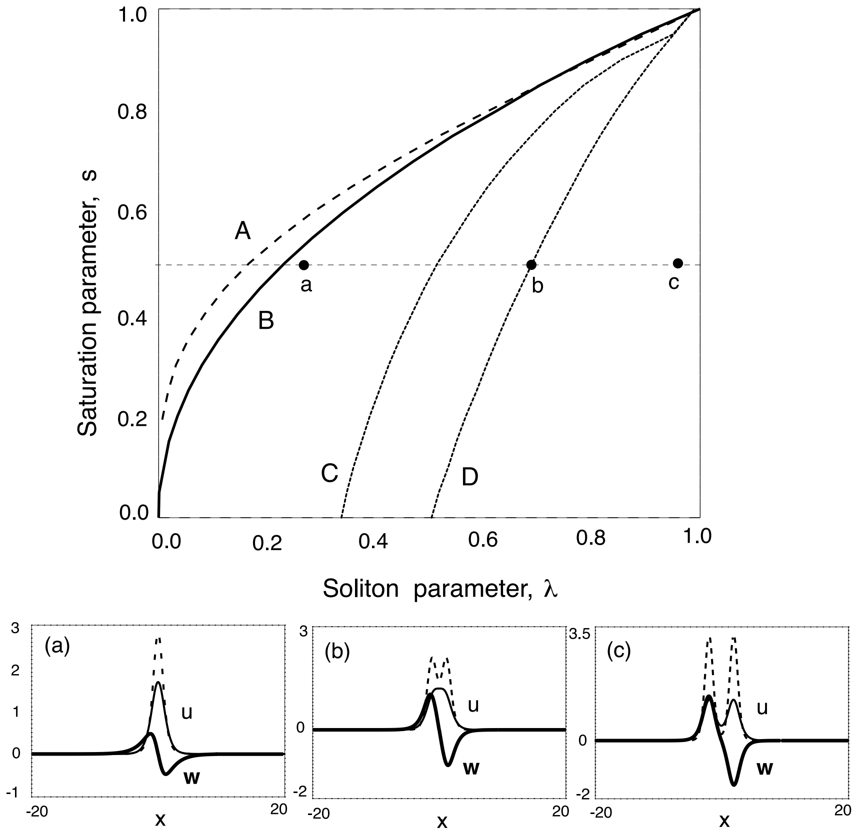

Figure 2. Threshold for the existence of two-component solitons composed of fundamental and first-order modes. Broken curve A: analytical estimates based on equation (6), full curve B: numerical calculations. Dotted curves: a threshold for two humps in the total intensity (curve C) and in the intensity of the u-component (curve D). (a)–(c) Amplitude (full curves) and total intensity (broken curves) profiles corresponding to the points a, b, and c at $s = 0.5$.

waveguide is wide enough to guide a two-node mode. However, even in the case when the linear bifurcation theory predicts that the soliton waveguide can only support a first-order mode, soliton solutions combining a zeroth-order mode in the u-component and a *second-order* mode in the w-component can still be found. They originate from more complex bifurcations described in [8] for the case of Kerr-like nonlinearity. The family of such solutions in our model is shown in figure 3, branch A-B-C.

Alternatively, multi-hump solitons can be formed as bound states of n solitons, when an effective waveguide supporting higher-order modes is created by n slightly overlapping fundamental solitons, with the total power n times greater than that of a single fundamental soliton. For instance, families of multi-hump solitons formed as bound states of n fundamental and first-order modes, resulting in $(2n-1)$-nodes amplitude profile of the w-component, exist in our model of the saturable nonlinearity even when the soliton-induced waveguide does not support a $(2n-1)$th mode. To demonstrate this effect of *soliton multiplication* (the term used in [8]) in a saturable medium, we numerically investigated the process of formation of bound states for different values of s. Figure 3 illustrates the soliton multiplication for $s = 0.5$ where, according to the bifurcation analysis, the effective waveguide created by the fundamental u-soliton admits only one, first-order, guided mode, as can be seen from figure 1. A family of the solitons with three nodes in the w-component (branch G-H-J in figure 3) appears at a soliton power greater than that of two independent, fundamental solitons. Such solitons, at small values of λ, are also *two-humped*. However, as λ approaches its limiting value, these solutions develop *four humps* in the intensity profile, as a result of deformation of the soliton waveguide created by the u-component, figure 3(J).

Following the soliton multiplication scenario, a family of the solitons with five nodes in the w-component (branch K-L-M in figure 3) appears at a soliton power greater than that of three independent, fundamental solitons. In the limit $\lambda \to 1$ this solution exhibits six humps in the intensity profile.

So far, we have discussed families of stationary solutions that have no nodes in the u-component profile. However, the model under consideration also admits soliton solutions composed of n bound, out-of-phase, solitons, 'glued' together by the first-order guided modes. Such solutions have $(n-1)$ nodes in the u-component transverse profile and n nodes in the w-component. An example of such a soliton is given in figure 3, branch D-E-F, for the case $n = 2$. With growing λ, these solitons evolve from having *two humps* in the intensity profile, similar to the low-power solutions of the branch G-H-J, to a three-humped shape, resembling the high-power solitons of the branch A-B-C.

The general conclusion that can be drawn from our analysis of the multi-soliton patterns formed by two interacting beams is that similar intensity distributions can

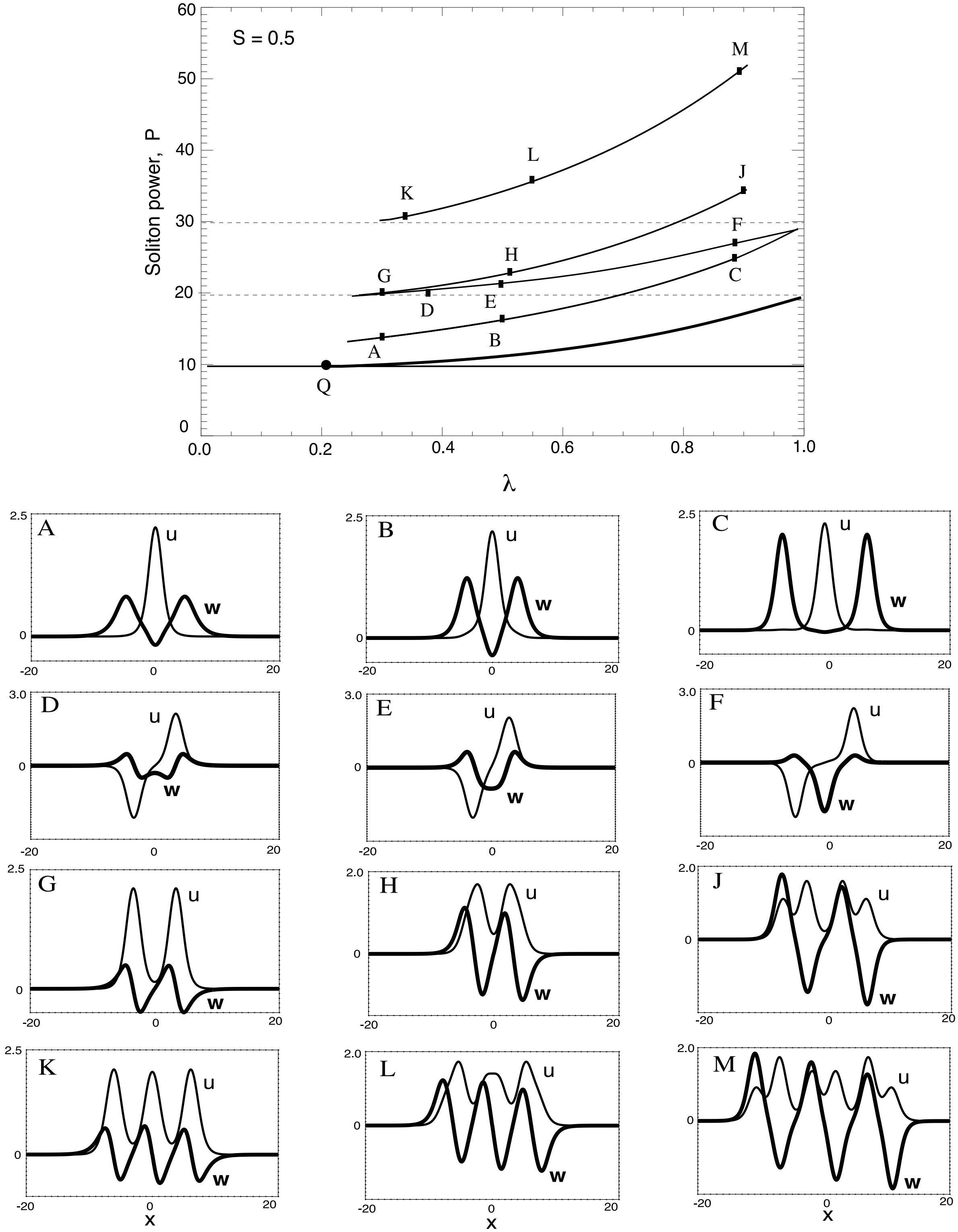

Figure 3. Examples of multi-hump soliton families at $s = 0.5$. Horizontal full line—fundamental soliton of the u-component bifurcating at the point Q. Heavy curve—solitons composed of fundamental and first-order modes. Branch A-B-C—solitons composed of fundamental and second-order modes. Solutions originating from a bound state of two (branch G-H-J) and three (branch K-L-M) in-phase fundamental solitons, each guiding a first-order mode in the w-component. Branch D-E-F—solutions originating from a bound state of two out-of-phase, fundamental solitons. Broken lines—total powers of two and three independent, fundamental solitons. Below: amplitude profiles of the u- and w-components corresponding to the points marked on the diagram.

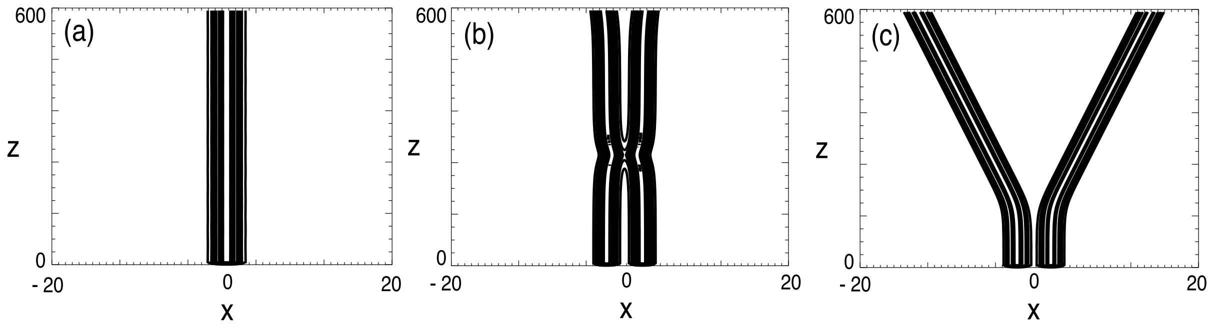

Figure 4. Examples of the propagation dynamics of two-component solitons at $s = 0.3$: (*a*) stable propagation at $\lambda = 0.2$, (*b*) propagation at $\lambda = 0.9$, and (*c*) unstable propagation at $\lambda = 0.95$. Initial solitons are members of the soliton family composed of fundamental (u) and first-order (w) modes shown in figures 2(*a*)–(c).

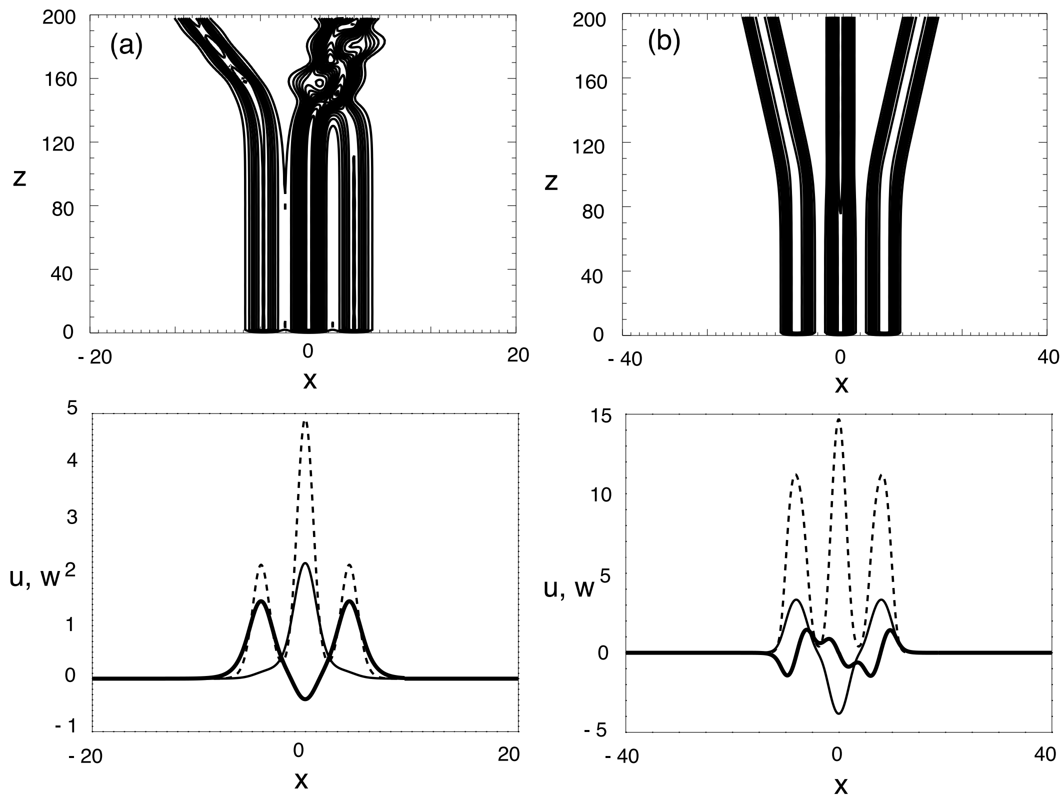

Figure 5. Examples of unstable propagation and modal structure of three-hump solitons at (*a*) $s = 0.5$, $\lambda = 0.64$, and (*b*) $s = 0.8$, $\lambda = 0.72$. Below: corresponding initial solitons at $z = 0$. Full light curves—amplitude of the u-component. Bold curves—amplitude of the w-component. Broken curves—total intensity profile.

be formed by different combinations of modes. According to the different modal structure, stationary solutions with the same number of humps exhibit totally different propagation dynamics, as we discuss below.

5. Propagation dynamics and soliton switching

We have investigated the dynamics of two-mode soliton states by solving the original evolution equations (2) numerically, using the split-step Fourier method. Since increasing λ means increasing the amplitude of the higher-order mode guided by a soliton-induced waveguide, we have analysed the effect of changing λ on the dynamics of the two-mode solitons. In this paper we are mainly concerned with the question of structural stability of multi-hump solitons and therefore we did not apply any perturbations to the initial conditions, which are taken as the exact stationary solutions of system (2) and evolve under action of numerical noise.

For the solitons composed of the zeroth and first-order modes (see figure 2), at low amplitudes of the antisymmetric component ($\lambda \to \lambda_1^{(0)}$), an initial one-hump soliton exhibits stable propagation. At higher amplitudes ($\lambda \to 1$), the initial two-hump soliton splits into two one-hump solitons. An example of the evolution of the intensity profiles for the members of the soliton family (*a*)-(*b*)-(*c*) in figure 2 is shown in figure 4. The soliton splitting occurs when the initial separation between the soliton humps is large enough. However, if a 'two-hump' soliton is formed as a bound state of two fundamental solitons both guiding the first-order modes (branch G-H-J in figure 3), they appear structurally unstable for any value of λ. The reason for this is quite simple: such solitons are formed with a separation between the humps already of the order that the soliton of the family (a)-(b)-(c) attains only at the limit of the existence domain, $\lambda \to 1$.

To illustrate the conclusion of the previous section, we compare propagation of two types of *three-hump* solitons. One of them is a member of a family A-B-C in figure 3, consisting of a zeroth and second-order modes and existing at low saturation, $s = 0.5$. Another one, at higher saturation $s = 0.8$, is formed from a bound state of three out-of-phase fundamental solitons, each of them guiding a first-order mode. The scenarios of the structural instability, developing as the two multi-hump solitons propagate through the medium, are drastically different. Depending on the structure of the two soliton components, the initial beam either splits into three single soliton-like beams, figure 5(b), or it exhibits a symmetry breaking instability, figure 5(a). The latter effect is similar to that earlier reported in [17] for the multi-hump solitons in quadratic media.

It seems to be a general feature of the multi-hump solitons to be structurally unstable to propagation, which opens up a possibility of using them in all-optical soliton switching. The two-component solitons with one-hump intensity profile, in contrast, exhibit seemingly steady propagation, as shown in figure 4(a), regardless of the complexity of their modal structure.

6. Conclusions

We have presented a theory of multi-hump solitary waves generated by incoherent interaction of two beams in a saturable optical medium. Families of the fundamental and multi-hump solitons have been found analytically, by means of the bifurcation analysis developed near a one-component soliton, and also numerically, using the relaxation technique. We have described several scenarios leading to the creation of multi-hump solitary waves which give birth to various spatially localized soliton patterns. We have also reported preliminary results on the structural instability of multi-hump solitary waves. A rigorous stability analysis of these solitons will be published elsewhere.

Acknowledgments

This work has been partially supported by the Australian Photonics Cooperative Research Centre. The authors are indebted to D Christodoulides, M Segev, D Skryabin and A Snyder for useful discussions, and to M Segev for a copy of [2] prior to its publication.

References

[1] See e.g. Segev M and Stegeman G 1998 *Phys. Today* **51** 42 and references therein
[2] Mitchell M, Segev M and Christodoulides D N 1998 *Phys. Rev. Lett.* **80** 4653
[3] Shih M, Chen Z, Mitchell M, Segev M, Lee H, Feigelson R S and Wilde J P 1997 *J. Opt. Soc. Am.* B **14** 3091
[4] Snyder A W, Hewlett S J and Mitchell D J 1994 *Phys. Rev. Lett.* **72** 1012
[5] Makhankov V G 1990 *Soliton Phenomenology* (Amsterdam: Kluwer) ch 8
[6] Zakharov V E and Rubenchik A M 1973 *Zh. Eksp. Teor. Fiz.* **65** 997 (Engl. transl. 1974 *Sov. Phys.–JETP* **38** 999)
[7] Pelinovsky D E, Afanasjev V V and Kivshar Yu S 1996 *Phys. Rev.* E **53** 1940
[8] Haelterman M and Sheppard A P 1994 *Phys. Rev.* E **49** 3376
[9] Calvalho M I, Singh S R, Christodoulides D N and Joseph R I 1996 *Phys. Rev.* E **53** R53
[10] Segev M, Valley G C, Singh S R, Carvalho M I and Christodoulides D N 1995 *Opt. Lett.* **20** 1764
[11] Manakov S V 1973 *Zh. Eksp. Teor. Fiz.* **65** 505 (Engl. transl. 1974 *Sov. Phys.–JETP* **38** 248)
[12] Kutuzov V, Petnikova V M, Shuvalov V V and V A Vysloukh 1998 *Phys. Rev.* E **57** 6056
[13] Christodoulides D N and Carvalho M I 1995 *J. Opt. Soc. Am.* B **12** 1628
[14] Davydov A S 1965 *Quantum Mechanics* (London: Pergamon) ch III
[15] Tratnik M V and Sipe J E 1988 *Phys. Rev.* A **38** 2011
[16] Malomed B A 1993 *Phys. Rev.* E **47** 2874
[17] Haelterman M, Trillo S and Ferro P 1997 *Opt. Lett.* **22** 84